PAPER

Analysis of High Frequency Noise of AlGaAs/GaAs HBT

Minseok KIM[†a)] ***and*** **Bumman KIM**[†], ***Nonmembers***

SUMMARY Hawkins noise model is modified for HBT application. The non-ideal ideality factor of HBT is included in both dynamic resistance and noise figure equations. Emitter resistance is also included. The extraction method of noise resistance R_n is developed. Based on the method, a simple analytic equation of R_n is derived and experimentally verified. The effects of noise sources on minimum noise figure are analyzed. The dominant noise sources are the shot noises of emitter and collector currents. Generally, when the minimum noise figure is measured at various current levels, there exists an current level at which the slope of minimum noise figure curve is zero. The zero slope current level coincides with the current level at which the noise contribution of the emitter and collector shot noises including the cancellation by correlation of two sources is minimum. Parasitic resistance degrades output noise through the shot noise amplification with a minor effect of the thermal noise of itself.
key words: *Hawkins model, minimum noise figure, noise resistance, ideality factor, correlation*

1. Introduction

Due to the low 1/f noise, high maximum oscillation frequency f_{max} and good linearity, AlGaAs/GaAs Heterojunction Bipolar Transistor(HBT) is emerging as a very useful device for a low phase noise oscillator and power amplifier at microwave and millimeter wave bands. As a device for low noise amplifiers, HBT has a poor minimum noise figure F_{min} than FET. Therfore, it could be assumed that HBT is not useful as a low noise device. But the noise figure of HBT is around 1 dB at mobile cellular/PCS band, which is quite usable. They have a lower optimum impedance, closer to 50 Ω and smaller noise resistance. Moreover, the current level for minimum F_{min} is about 1 mA, which is much lower than FET. Due to these favorable characteristics, HBT is a very promising low noise device at a low operation frequency range(which is less than about 5 GHz).

Hawkins model[1] is a simple noise model for Si-BJT. This model includes the analytic expressions for noise figure and optimum source impedance. The high frequency noise model[2]–[4] of HBT is a little different from that of Si-BJT. But the difference mainly stems from the higher operation frequencies of HBT than those of Si-BJT. Within a low frequency range at which HBT is applicable to low noise device, however, it is possible to describe the noise characteristics of HBT using the noise models of Si-BJT with minor modifications. This paper proposes a modified Hawkins model for HBT noise analysis. A method for the extraction of noise resistance R_n from Hawkins model is also developed. Using the new extraction method and modified analytic equation of noise figure, the R_n is calculated and compared with measured results. We have also analyzed the effect of noise sources on F_{min} using the modified Hawkins noise model with correlated emitter and collector shot noise sources.

Manuscript received September 17, 1998.
†The authors are with the Department of Electronics and Electrical Engineering, Pohang University of Science and Technology, San 31 Hyojadong, Nam-Gu, Pohang, Kyungbuk, Korea.
a) E-mail: mskim@shiloam.postech.ac.kr

2. Modified Noise Model for HBT

2.1 Modified Hawkins Model

A simple noise equivalent circuit of Si-BJT is shown in Fig. 1(a) where i_e emitter current shot noise source, i_c collector current shot noise source, e_{rb} thermal noise source due to base resistance(R_b), e_{re} thermal noise source due to emitter resistance(R_e), C_{TE} junction capacitance, $r_e(=kT/qI_E)$ dynamic resistance, α common base current gain. α is a single pole function of the form

$$\alpha = \frac{\alpha_0}{1 + jf/f_b'} \tag{1}$$

where α_0 common base current gain at D.C., f_b' cut-off frequency of base transit time(τ_b) plus base-collector depletion layer transit time(τ_c). The form of single pole function of Eq. (1) is valid within a low operation frequency range($\omega\tau_c < 0.5$). Actually, in Si-BJT, f_b' was the cut-off frequency f_b of only base transit time because base transit time of Si-BJT was normally much larger than base-collector depletion layer transit time. It is somewhat inconvenient to use the equivalent circuit of Fig. 1(a) in which emitter and collector shot noise sources are strongly correlated. To avoid the complexity of the noise model, in Fig. 1(b), the correlated shot noise sources i_e and i_c are transformed to the uncorrelated noise sources e_e and i_{cp} given by [5].

$$\overline{e_e^2} = 2kTr_e \tag{2}$$

$$\overline{i_{cp}^2} = \frac{2kT(\alpha_0 - |\alpha|^2)}{r_e} \tag{3}$$

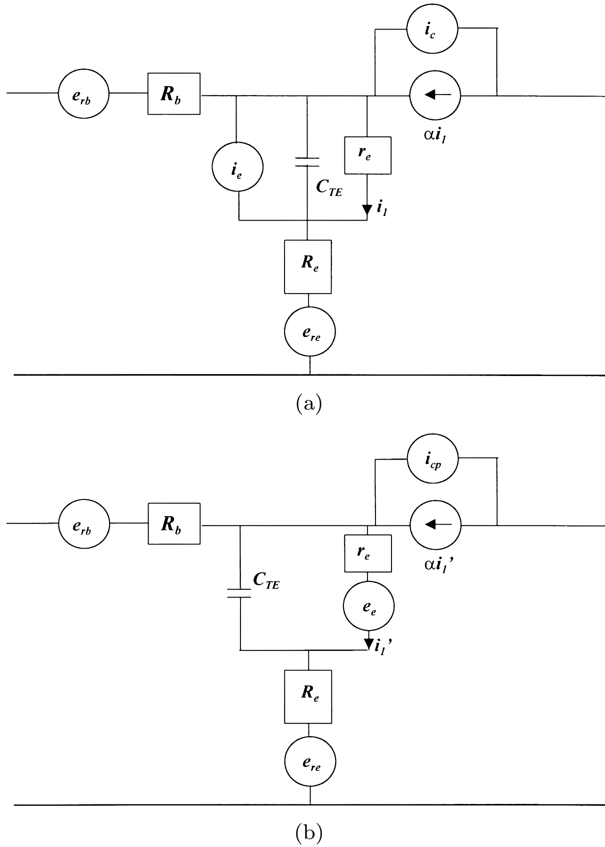

Fig. 1 Simple noise equivalent circuit (a) with correlated noise sources i_e and i_c, (b)with uncorrelated noise sources e_e and i_{cp}.

$$r_e = kT/qI_E \tag{4}$$

Hawkins model uses the equivalent circuit of Fig. 1(b) without emitter resistance.

In order to use Hawkins noise model for HBT, the characteristic difference of HBT from Si-BJT must be considered. First, the non-ideal ideality factor of HBT must be included accurately for both dynamic resistance and noise source equations. Considering ideality factor n_e of HBT, Eqs. (2)–(4) for Si-BJT are transformed to following forms:

$$\overline{{e_e}^2} = 2n_e kTr_e \tag{5}$$

$$\overline{{i_{cp}}^2} = \frac{2n_e kT(\alpha_0 - |\alpha|^2)}{r_e} \tag{6}$$

$$r_e = n_e kT/qI_E \tag{7}$$

Second, the effect of series emitter resistance R_e on the noise figure must be included [2]. Because of the small emitter size and small base resistance, the emitter resistance effect on noise figure is not negligible. After some manipulation, analytic expressions for noise figure and optimum source impedance of HBT are extracted as follows.

$$F_{min} = \frac{n_e a(R_b + R_e + R_{opt})}{r_e} + \frac{n_e \alpha_0}{|\alpha|^2} + (1 - n_e) \tag{8}$$

$$X_{opt} = \frac{\alpha_0}{|\alpha|^2}\frac{\omega C_{TE}{r_e}^2}{a} \tag{9}$$

$$\begin{aligned} {R_{opt}}^2 = {} & (R_b + R_e)^2 - {X_{opt}}^2 \\ & + \frac{\alpha_0}{|\alpha|^2}\frac{r_e(2(R_b + R_e) + r_e)}{a} \\ & + \frac{2r_e(R_b + R_e)(1 - n_e)}{n_e a} \end{aligned} \tag{10}$$

$$a = \frac{\alpha_0}{|\alpha|^2} - 1 + \frac{\alpha_0}{|\alpha|^2}(\omega C_{TE} r_e)^2 \tag{11}$$

Our modified Hawkins model for HBT, Eqs. (8)–(11), may seem to be the same as Costa model [2] or Chen model [6]. But there are obvious differences between our model and the other models. Chen replaced base transit time cut-off frequency f_b of original Hawkins model with total transit time cut-off frequency f_T. Except this replacement, Chen's expressions for noise parameters are the same as original Hawkins model for Si-BJT. But, in the view of equivalent circuit theory, f_b' must be used in the noise model of recent HBT. Costa model also used f_T and included emitter resistance. But he included non-ideal ideality factor n_e in dynamic resistance only. However, non-ideal ideality factor n_e must be considered in both dynamic resistance and noise source. So, We have propely considered non-ideal ideality factor n_e and cut-off frequency f_b' for the noise model of recent HBT which has similar transit times of base layer and base-collector depletion layer.

2.2 Extraction of Noise Resistance from Hawkins Model

The noise resistance R_n was not considered in the original Hawkins model. To extract R_n from Hawkins model, R.A.Pucel [7] employed correlation matrix and the procedure is complex. In this paper, we present a simple and direct method for extraction of R_n from Hawkins model.

A chain representation of a noisy network is shown in Fig. 2(a) where e_n equivalent noise voltage generator, i_n equivalent noise current generator, e_s thermal noise generator due to the real part(R_s) of input source impedance Z_s. A chain representation of Fig. 2(a) may be converted to the equivalent circuit shown in Fig. 2(b), where e_{ni} is the equivalent noise voltage generator of the input circuit:

$$e_{ni} = e_s + e_n + Z_s i_n \tag{12}$$

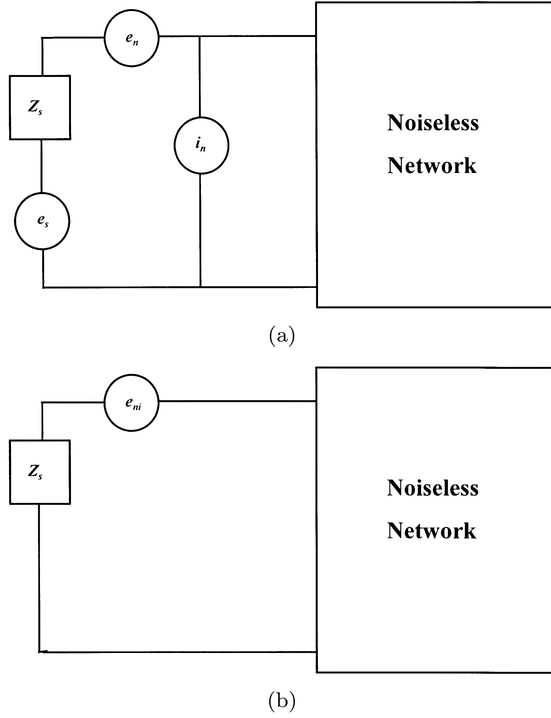

Fig. 2 Equivalent circuits of noisy network. (a)Chain representation. (b)Converted chain representation.

$$\overline{e_{ni}^2} = \overline{e_s^2} + \overline{e_n^2} + \overline{i_n^2}|Z_s|^2 + 2Re[Z_s\overline{i_n e_n^*}] \quad (13)$$

The current generator i_n, which is partially correlated with e_n, is split into an uncorrelated current i_u and a fully correlated current i_c.

$$i_c = Y_c e_n \quad (14)$$

$$i_n = i_u + Y_c e_n \quad (15)$$

$$\overline{i_n e_n^*} = \overline{i_u e_n^*} + Y_c\overline{e_n e_n^*} = Y_c\overline{e_n^2} \quad (16)$$

where Y_c=G_c+jB_c is a correlation admittance. From Eqs. (12)–(16), e_{ni} can be expressed as follows:

$$\begin{aligned}\overline{e_{ni}^2} &= \overline{e_s^2} + \overline{e_n^2} + \overline{i_n^2}|Z_s|^2 + 2Re[Z_s\overline{i_n e_n^*}] \\ &= \overline{e_s^2}+\overline{e_n^2}+\overline{i_n^2}|Z_s|^2+2[(R_sG_c-X_sBc)\overline{e_n^2}]\end{aligned} \quad (17)$$

Thus, it is possible to extract R_n using following relationship:

$$\overline{e_{ni}^2}|_{Z_s=0} = \overline{e_n^2} = 4kTR_n \quad (18)$$

Note that e_{ni} can be directly derived from the expression for noise figure.

$$F = \frac{\overline{e_{ni}^2}}{\overline{e_s^2}} \quad (19)$$

Using above Eqs. (18) and (19) and the equation for noise figure of our modified Hawkins model, R_n can be directly extracted as follows:

$$\begin{aligned}R_n = R_b+R_e+\frac{n_e r_e}{2}+\left(\frac{\alpha_0}{|\alpha|^2}-1\right)\frac{n_e(R_b+R_e+r_e)^2}{2r_e} \\ +\frac{\alpha_0}{|\alpha|^2}\frac{n_e}{2r_e}(\omega C_{TE} r_e(R_b+R_e))^2\end{aligned} \quad (20)$$

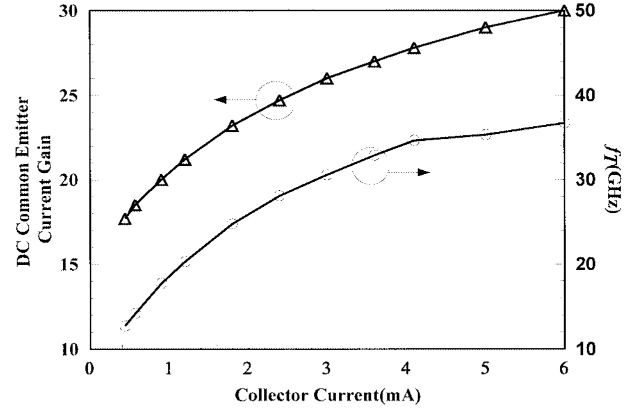

Fig. 3 Measured common emitter current gain and cut-off frequency for our AlGaAs/GaAs HBT with V_{CE} = 2 V.

3. Experimental Results

A 3 × 20 μm^2 emitter finger self-aligned AlGaAs/GaAs HBT with abrupt junction was fabricated and evaluated. The epitaxial structure consists of a 800 Å InGaAs contact layer(n = 1.0 × 10^{19} cm^{-3}), a 1200 Å GaAs cap layer (n = 5.0 × 10^{18} cm^{-3}), a 1000 Å AlGaAs emitter layer (n = 2.0 × 10^{17} cm^{-3}), a 1000 Å GaAs base layer (p = 2.0 × 10^{19} cm^{-3}), a 4000 Å GaAs collector layer (n = 2.0 × 10^{16} cm^{-3}), a 6000 Å GaAs subcollector layer (n = 5.0 × 10^{18} cm^{-3}) on a semi-insulating GaAs substrate.

The AuGe/Ni/Au and Pt/Ti/Pt/Au metal system[8] are used for emitter and self-aligned base electrode. The specific contact resistance of base contact was measured to be 3.0 × 10^{-6} Ω cm^2. The device had base and collector current ideality factors of n_b=1.37 and n_c=1.23, respectively. The ideality factor of emitter current n_e was 1.29. On-wafer s-parameter measurements was performed using HP8510C network analyzer. As shown in Fig. 3, the device has a common emitter current gain of 30 and a total transit time cut-off frequency f_T of 36 GHz at a collector current of I_C=6 mA. A base resistance of R_b = 15 Ω, a series emitter resistance of R_e = 2.5 Ω were exracted from the s-parameter data.

To calculate noise parameters, it is necessary to accurately extract circuit parameters. The circuit parameters for noise modeling were derived as follows. The common base current gain at D.C. α_0 and ideality factor n_e were extracted from the Gummel plot. The

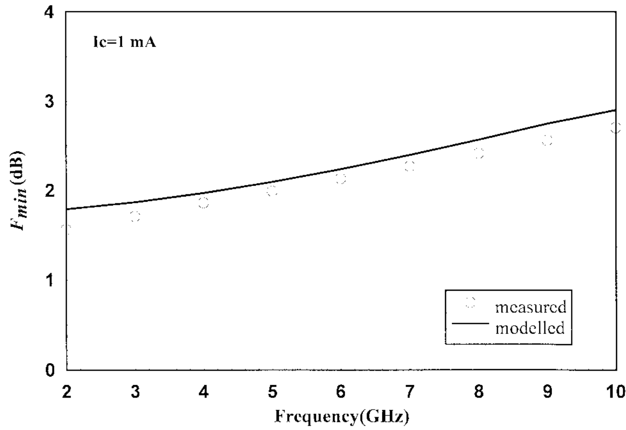

Fig. 4 Minimum noise figure versus frequency of our AlGaAs/GaAs HBT at $I_C = 1$ mA.

dynamic resistance r_e was also derived from the emitter current level and n_e. Junction capacitance C_{TE} and cut-off frequency f_b' were derived from the curve $1/(2\pi f_T)$ against $1/I_C$. This extraction method for C_{TE} and f_b' was also proposed in Ref. [1],[9]. The extracted value of C_{TE} was a function of bias and 0.16 pF at $I_C = 6$mA. The extracted f_b' was 45.8 GHz. Base resistance R_b was obtained from the method described in Ref. [10]. To calculate R_b using the resistance model, it is necessary to know specific contact resistance of base contact and exact emitter width considering lateral under-cut depth under the emitter electrode. We have measured lateral under-cut depth under emitter electrode by SEM and specific contact resistance of base electrode by TLM pattern. The calculated value of R_b from the base resistance model was about 15 Ω which was agreed with the extracted value of R_b from s-parameters.

The noise figure were measured using a HP 8970A noise figure meter and FOCUS tuner. Figure 4 shows the noise figure vs. frequencies, calculated from our model and measured ones at $I_C = 1$ mA. As shown, our model traced the measurement data very well. To further investigate the current dependence of noise figure, Figure 5 shows the calculated and measured noise figure vs. emitter current. As shown in Fig. 5(a), F_{min} of our modified Hawkins model agrees very well with the measurement. But Costa model overestimates F_{min} at a low current and underestimates at a high current. We assume that the overestimation at a low current is due to the replacement f_b' with f_T, because f_T is a lot lower than f_b' at a low current, while the two frequencies become similar at a high current. The underestimation at a high current is due to the ideal n_e in noise figure equation of Costa model. As shown in Fig. 5(b) and (c), R_{opt} and X_{opt} obtained from the two models did not trace the measured values very well. This is the drawback of Hawkins model. We assume this is due to the simple Hawkins model in which many parasitic circuit elements are not included. Specially, the optimum noise susceptance resulting from simple noise model without external base-collector capacitance C_{bc}' does not agree well with the measurement data[11]. As shown in Fig. 5(d), the calculated R_n using Eq. (20) agrees very well with measurement. Therefore, we could verify our extraction method of R_n.

4. Effect of Noise Source on F_{min}

In Hawkins model, to avoid complexity of calculation of F_{min} due to the correlation between emitter and collector shot noise sources, the correlated shot noise sources i_e and i_c are transformed to the equivalent uncorrelated noise sources e_e and i_{cp}. However, to investigate the F_{min} dependence on the noise sources, it is more efficient to use i_e and i_c instead of e_e and i_{cp}. The noise figure F for HBT using i_e and i_c was derived using equivalent circuit of Fig. 1(a).

$$\begin{aligned} F \;=\; & 1+\frac{(R_b+R_e)}{R_s}+\frac{n_e}{2R_s r_e}\left[(R_s+R_b+R_e)^2+{X_s}^2\right] \\ & +\frac{\alpha_0}{|\alpha|^2}\frac{n_e}{2R_s r_e}\begin{pmatrix}(R_s+R_b+R_e+r_e(1-\omega C_{TE}X_s))^2\\ +(X_s+\omega C_{TE}(R_s+R_b+R_e))^2\end{pmatrix} \\ & -\frac{n_e}{R_s r_e}\left[(R_s+R_b+R_e+r_e)(R_s+R_b+R_e)+{X_s}^2\right] \end{aligned} \tag{21}$$

where R_s and X_s the input source impedance terms. The 2nd term in Eq. (21) is due to the base thermal noise e_{rb} and emitter thermal noise e_{re}, the 3rd term due to the emitter shot noise, the 4th term due to the collector shot noise, and the 5th term due to the correlation [12] between the emitter and collector shot noise sources. The calculated minimum noise figure using Eq. (21) is identical to the results of Eq. (8) using uncorrelated noise sources e_e and i_{cp}. Therefore, we could know that the correlation between emitter and collector noise sources was actually included in Hawkins model.

Using the terms in noise figure equation (21) with optimum noise matching condition, the contribution of each noise sources to the minimum noise figure at 4 GHz has been calculated and depicted in Fig. 6. As shown in Fig. 6(a), comparing the noise due to the total noise sources with that due to the thermal noise sources, we know that the shot noise sources are the dominant term. The noise figure due to the each shot noise sources are much higher than that due to the total shot noise sources. However, the correlation factor of the two shot noises are almost -1 and they are canceling out almost exactly. As a result, noise figure due to the total shot noise sources(i_e, i_c, and correlation) is much smaller than that due to the each shot noise source. The correlation between the shot noise sources is stronger at a higher current level, and the noise due to the correlation increases strongly as current increases. Figure 6(b) shows the noise figure due to the total shot

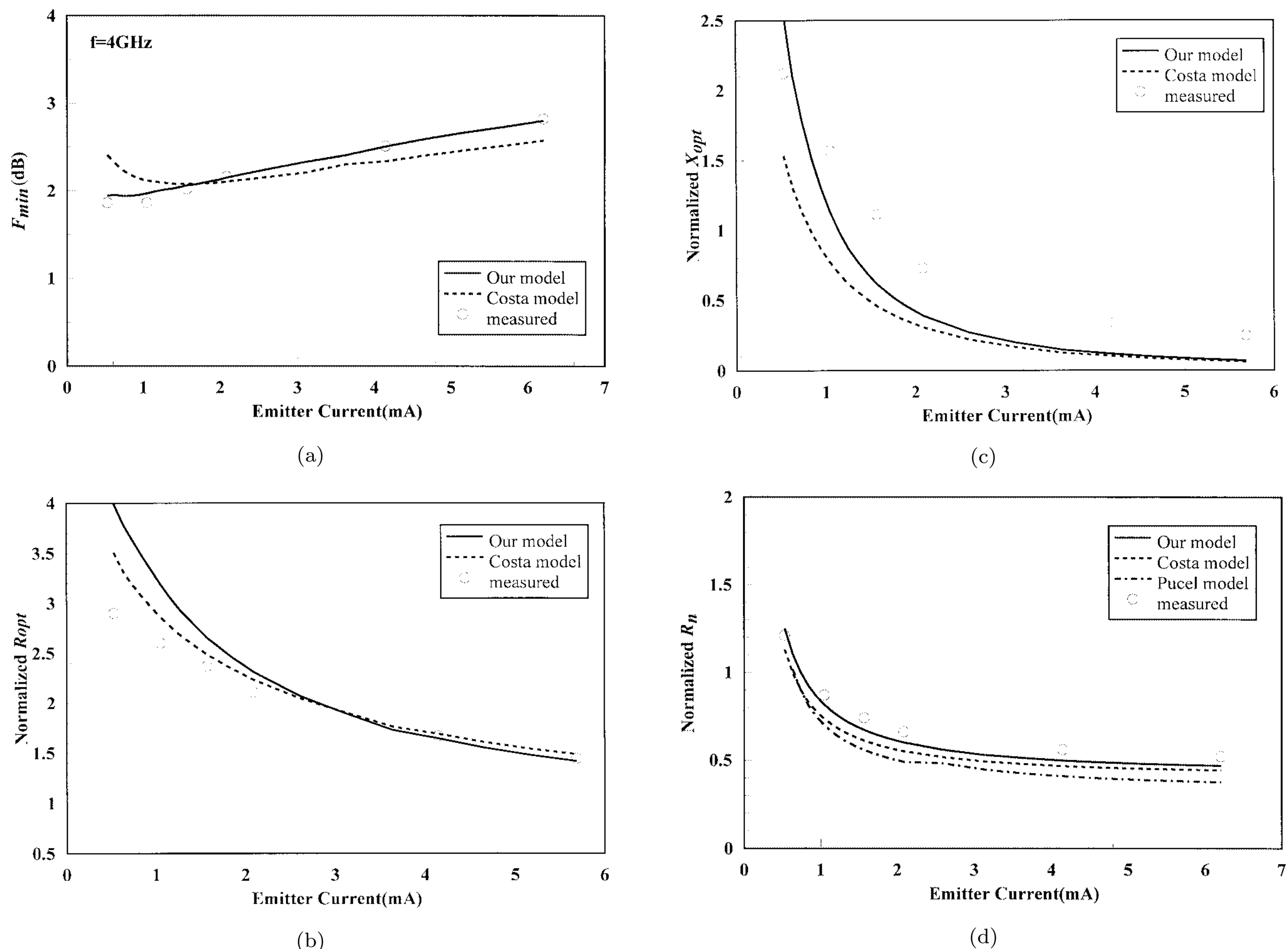

Fig. 5 Noise parameters versus emitter current of our AlGaAs/GaAs HBT at 4 GHz with V_{CE} = 2 V. (a)Minimum noise figure F_{min}(dB). (b)Normalized R_{opt} to 50 Ω. (c)Normalized X_{opt} to 50 Ω. (d)Normalized noise resistance R_n to 50 Ω.

noise sources and the thermal noise sources. Due to the reduced correlation at a low current level, there is a current level at which the noise figure coming from the total shot noise sources(i_e, i_c, and correlation) is minimum. This current level (I_{min}) agrees with the current at which noise figure due to the total noise sources(i_e, i_c, correlation and thermal noises) is minimum. The terms of noise figure due to the thermal noise sources increases with current.

Figure 7 compares the calculated F_{min} due to the each noise source. The complete noise model model-21 (see Eq. (21)) accurately predicts measured noise figure. The model- 22 is the output noise due to the total shot noise sources(i_e, i_c, and correlation) with $R_e+R_b \neq 0$ (the output noise without the *thermal noise sources*), the model-23 due to the total shot noise sources with $R_e=R_b=0$. Comparing model-21 with model-22, we know that F_{min} due to the thermal noise sources increases with current. Comparing model-22 with $R_e+R_b \neq 0$ and model-23 with $R_e=R_b=0$, we found that F_{min} of model-22 is higher than that of model-23. The higher F_{min} of model-22 is due to the shot noise amplification by R_e+R_b. Therefore, we conclude that base and emitter resistances degrade output noise through the shot noise amplification with a lesser important effect of the thermal noise itself. This amplification effect of R_e+R_b is seen once more from the result of comparison model-11 with model-12. The model-12(with $R_e=R_b=0$, $i_e=0$, $i_c \neq 0$) have approximately constant value of F_{min} versus current. However F_{min} of the model-11(with $R_e+R_b \neq 0$, $i_e=0$, $i_c \neq 0$) is not only higher than model-12 but also increases with current. It is due to the shot noise amplification effect of R_e+R_b and the increased thermal noise with current. We have seen a quite similar behavior for emitter shot noise sources in our model.

5. Conclusions

We have proposed the modified Hawkins model for HBT. First, non-ideal ideality factor of HBT is considered in both dynamic resistance and noise figure derivation in our model. Second, we have used cut-off

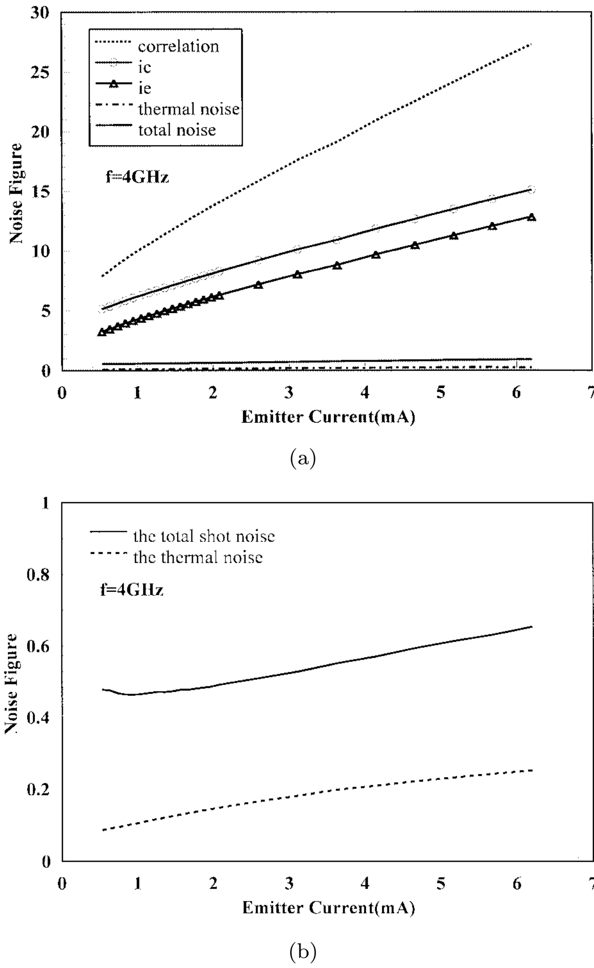

Fig. 6 Contribution of each noise sources to minimum noise figure. The curves are extracted from the each terms of noise figure equation (21) under the condition of optimum noise matching. (a)noise figure due to each noise sources. (b)noise figure due to total shot noise sources (i_e, i_c and correlation) and thermal noise sources.

frequency f_b' of base transit time combined with base-collector depletion layer transit time. New extraction method of R_n was also proposed. R_n is directly derived from noise figure equation in our model and it has been experimentlly verified.

We have analyzed the effect of noise sources on F_{min} of AlGaAs/GaAs HBT using our modified Hawkins model with i_e and i_c instead of e_e and i_{cp}. We found the dominance of shot noise sources and the amplification effect of R_e+R_b. Parasitic resistance degrades output noise through the shot noise amplification with some thermal noise contribution. The correlation coefficient of shot noise sources is approximately -1. The noise contribution of thermal noise source increases with current. The current level for the minimum F_{min} coincides with the current level at which output noise due to the total shot noise sources is minimum.

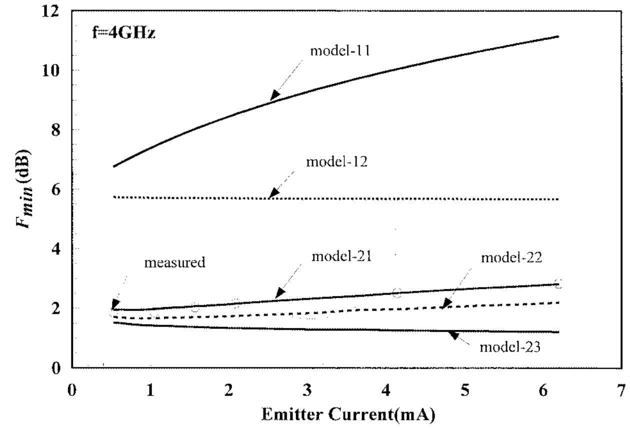

Fig. 7 Minimum noise figure calculated from the model with each noise sources (i_e, i_c, thermal noise sources) and parasitic resistance (R_e+R_b) for our AlGaAs/GaAs HBT at 4 GHz and V_{CE}=2 V;
model-11 : F_{min} with $i_e = 0$, $i_c \neq 0$, $R_e+R_b \neq 0$,
model-12 : F_{min} with $i_e = 0$, $i_c \neq 0$, $R_e = R_b = 0$,
model-21 : F_{min} with $i_e \neq 0$, $i_c \neq 0$, $R_e+R_b \neq 0$,
model-22 : F_{min} with $i_e \neq 0$, $i_c \neq 0$, $R_e+R_b \neq 0$,
(the output noise without the *thermal noise sources*)
model-23 : F_{min} with $i_e \neq 0$, $i_c \neq 0$, $R_e = R_b = 0$.

Acknowledgement

This work has been partially supported by Agency for Defense Development.

References

[1] R.J. Hawkins, "Limitations and Nielsen's and related noise equations applied to microwave bipolar transistor, and a new expression for the frequency and current dependent noise figure," Solid State Elect., vol.20, pp.191–196, 1977.
[2] D. Costa, "Impact of Al compoition on RF noise figure of AlGaAs/GaAs heterojunction bipolar transistors," IEEE Trans. Electron Devices, vol.ED-42, pp.2043–2046, 1995.
[3] T. Daniel, "Bias and temperature dependent noise modeling of HBTs," IEEE MTT-S Digest, pp.1469–1472, 1997.
[4] J.J. Liou, T.J. Jenkins, L.L. Liou, R. Neidhard, D.W. Barlage, R. Fitch, J.P. Barrette, M. Mack, C.A. Bozada, R.H.Y. Lee, R.W. Dettmer, and J.S. Sewel, "Bias, frequency, and area dependencies of high frequency noise in AlGaAs/GaAs HBT's," IEEE Trans. Electron Devices, vol.ED-43, pp.116–122, 1996.
[5] A. Van Der Ziel, "Noise in solid state devices and circuits," John-Wiley & Sons, 1986.
[6] Y.K.Chen, R.N. Nottenburg, R.A. Hamm, and D.A. Humphery, "Microwave noise performance of InP/InGaAs heterostructure bipolar transistors," IEEE Trans. Electron Devices Lett., vol.EDL-10, pp.470–472, 1989.
[7] R.A. Pucel and U.L. Rohde, "An exact expression for the noise resistance R_n for the Hawkins bipolar noise model," IEEE Microwave and Guided Wave Lett., vol.3, pp.35–37, 1993.
[8] H. Okada, S. Shikata, and H. Hayashi, "Electrical characteristics and reliability of Pt/Ti/Pt/Au ohmic contacts to p-type GaAs," J.J. Appl. Phys., vol.30, pp.L558–L560, 1991.

[9] H. Schumacher, U. Erben, and A. Gruhle, "Noise characterisation of Si/SiGE heterojunction bipolar transistors at microwave frequencies," Electron. Lett., vol.28, pp.1167–1168, 1992.
[10] H.F. Cooke, "Microwave transistor: Theory and design," Proc. IEEE, vol.59, pp.1163–1181, 1971.
[11] L. Escotte, J.P. Roux, R. Plana, J. Graffeuil, and A. Gruhle, "Noise modeling of microwave heterojunction bipolar transistors," IEEE Trans. Electron Devices, pp.883–889, 1995.
[12] A. Van Der Ziel and A.G.T. Becking, "Theory of junction diode and junction transistor noise," Proc. IRE., pp.589–594, 1958.

Minseok Kim received the B.S. degree in electronics engineering from Sungkyunkwan University, Seoul, KOREA, in 1993, and the M.S. degree in electronics and electrical engineering from Pohang University of Science and Technology, Pohang, KOREA, in 1995. His research areas are high frequency noise modeling of AlGaAs/GaAs HBT and low noise device design.

Bumman Kim received the Ph.D. degree in electrical engineering from Carnegie-Mellon University, Pittsburgh, PA, in 1979. From 1978 to 1981, he was engaged in fiber-optic component research at GTE Lab. Inc. In 1981, he joined the Central Research Lab. of Texas Instruments, Inc., where he was involved in development of GaAs power FET's and monolithic microwave integrated circuits. He has developed a large signal model of a power FET, dual-gate FET's for gain control, and high-power distributed amplifiers, and various millimeter-wave MMIC's. In 1989, he joined Pohang University of Science and Technology, Pohang, KOREA, where he is a Professor in the Electronics and Electrical Engineering Department, and Director of the Microwave Application Research Center, working on device and circuit technology for MMIC's. He has published over 100 technical papers in this area. Dr. Kim is a member of Korean Academy of Science and Technology.